Current-year shoot hydraulic structure in two boreal conifers – implications of growth habit on water potential

Annikki Mäkelä*), Leila Grönlund, Pauliina Schiestl-Aalto, Tuomo Kalliokoski, Teemu Hölttä

Faculty of Agriculture and Forestry / Institute of atmospheric research and earth system science; P.O.Box 27 (Latokartanonkaari 7); 00014 University of Helsinki

*) corresponding author, tel: +358 41 5106515, email: annikki.makela@helsinki.fi

Key words: conduit diameter, hydraulic structure, *Picea abies*, *Pinus sylvestris*, shoot allometry, shoot shape, water potential gradient

Running head: Shoot hydraulic structure and water potential

Abstract

Metabolic scaling theory allows us to link plant hydraulic structure with metabolic rates in a quantitative framework. In this theoretical framework, we considered the hydraulic structure of current-year shoots in *Pinus sylvestris* and *Picea abies*, focusing on two properties unaccounted for by metabolic scaling theories: conifer needles are attached to the entire length of shoots, and the shoot as a terminal element does not display invariant properties. We measured shoot length and diameter as well as conduit diameter and density in two locations of 14 current year non-leader shoots of pine and spruce saplings, and calculated conductivities of shoots from measured conduit properties. We evaluated scaling exponents for the hydraulic structure of shoots at the end of the water transport pathway from the data and applied the results to simulate water potential of shoots in the crown. Shoot shape was intermediate between cylindrical and paraboloid. Contrary to previous findings, we found that conduit diameter scaled with relative, not absolute, distance from the apex and absolute under-bark shoot diameter independently of species within the first year shoots. Shoot hydraulic conductivity scaled with shoot diameter and hydraulic diameter. Larger shoots had higher hydraulic conductance. We further demonstrate by novel model calculations that ignoring foliage distribution along the hydraulic pathway overestimates water potential loss in shoots and branches and therefore overestimates related water stress effects. Scaling of hydraulic properties with shoot size enhances apical dominance and may contribute to the decline of whole-tree conductance in large trees.

Introduction

The metabolic rate of trees is very tightly linked to xylem hydraulic conductance, i.e., to the rate at which xylem can supply the leaves with water. A proper understanding of tree water relations therefore requires that we link whole-tree anatomical and structural properties with their physiological function (Zimmermann 1983). However, despite a long tradition of research into both the hydraulic structure of trees (e.g., Huber 1928, Zimmermann 1983) and into tree metabolic rates (e.g. Kozlowski et al. 1991), it seems that it was only the invent of the metabolic scaling theory (West et al. 1999) that allowed us to start merging these aspects in a quantitative framework. While the original WBE scaling model was introduced as a "zero order model" including many simplifications, more recent developments of the theory have incorporated more detailed structural assumptions (Savage et al. 2010), and species-specific parameterisations have allowed for a representation of species differences (Sperry et al. 2012). On the other hand, the obvious simplification of the scaling models that assumes crowns as symmetrical entities where leaves are attached solely to the distal ends of the branches at the end of the water transport pathway has so far not been contested nor has its quantitative significance been explored.

Many boreal conifer species manifest strong apical dominance, with the stems growing straight upward and the growth of the branch declining downward to produce rather narrow and slender crowns (Oliver and Larson 1996). As already observed by Huber (1928), the foliage mass to xylem cross-sectional area of branches and stem increases from the top downward, and the leaf-specific conductivities of sapwood are larger along the stem than in the lateral branches (Zimmermann 1983, Lintunen and Kalliokoski 2010). This has been interpreted as a contribution to apical dominance, as it makes the leader more readily supplied by xylem transport than the lateral branches (Zimmermann 1983, Tyree et al. 1991). Consistently with this pattern, the new shoots at the branch tips decrease in size from top down in trees showing apical dominance even under unshaded conditions (e.g. Nikinmaa et al. 2003). At the same time, conduit diameter and consequently the

hydraulic conductivity of the xylem in new shoots has been found to decrease with decreasing shoot length and diameter (Grönlund et al. 2016). From the point of view of metabolic scaling theory this suggests that crowns of conifers with apical dominance cannot be regarded as regular, self-similar fractals.

The hydraulic properties of the new shoots at the end of the hydraulic pathway are important as hydraulic resistance is a significant determinant of leaf gas exchange (Brodribb 2009), and the new shoots constitute a large part of the total resistance in the tree hydraulic pathway from soil to leaf (Tyree et al. 1991). The allometric scaling theory (West et al. 1999, Savage et al. 2010) suggests that the diameter of the hydraulic conduits scales with both distance from the branch apex (Mencuccini et al. 2007, Petit et al. 2008) and branch / stem diameter (Savage et al. 2010, Jyske and Hölttä 2015). That the hydraulic properties of new shoots scale with shoot dimensions (Grönlund et al. 2016) seems consistent with these results. However, the wide variability of shoot size within the crown prompts the question of how to interpret the shoot in relation to the "size-invariant terminal twig", a basic concept underlying the scaling theory (West et al. 1999, Savage et al. 2010). Should the shoots themselves be considered as the terminal twigs? The "terminal twig" should then be allowed to vary in size. Alternatively, should the "terminal twig" be defined in a more abstract manner? The answer to these questions would depend on the scaling of hydraulic properties with individual shoot dimensions.

The assumption of the scaling model that the transpiring leaves are attached to the apex of the terminal twigs (West et al. 1999, Savage et al. 2010) is a reasonable simplification at the scale of the entire crown. Focusing on shoot internal structure, we must note that foliage in general, and most evidently conifer needles, are attached to the entire length of shoots, not just to the apex. This is the case also further down along the water transport pathway as needles are kept on branches for several growing seasons (Ewers and Schmid 1981, Ťupek et al. 2015). If all needles are transpiring, the total water flux should decrease along the pathway even in the absence of branching junctions. This could have implications for the structure and hydraulic properties of conifer shoots and possibly for those of entire trees.

From an evolutionary point of view, shoot structure should be functionally efficient with minimum investment of resources (McCulloh et al. 2003). A minimum investment in shoot structure from the point of view of water transport could be achieved if shoot and conduit widening from tip to base corresponded with the extraction of water by transpiration along the length of the shoot. The foliage distribution as well as the environmental drivers of transpiration appear fairly evenly distributed across the shoot axis. This would create a uniform outflow of water from the shoot to the needles, implying a linear decline of water flux from base to apex. If all of this decline was compensated for by adjustment of shoot cross-sectional area, this would also decline linearly from base to apex, meaning that distance from the apex (x) is proportional to diameter ($D(x)$) squared, which defines a parabolic relationship ($x \propto D(x)^2$). Assuming that shoot shape is a solid of revolution defined by this parabola gives rise to paraboloid shape of the shoot (see Figure 1).

On the other hand, any possible hydraulic benefits of strongly widening terminal shoots might be lost in additional construction costs the following year when daughter shoots need to be built from buds at the tip of the previous year's shoot. Both mechanical support of the daughter shoots, and efficient water transport to them already in the early season when secondary growth has not been completed or even started, would seem to benefit from a fairly cylindrical shoot structure, such as the idealised terminal twig structure assumed in the scaling theory (West et al. 1999, Savage et al. 2010, Figure 1). In this case, however, the shoot internal structure, including the size and number of conduits and the fraction of conducting to total cross-sectional area, would have to be adjusted accordingly in view of the extraction of water along the shoot axis.

Our objective is to explore shoot and xylem conduit features of current-year shoots of two conifers, Scots pine (*Pinus sylvestris* L) and Norway spruce (*Picea abies* (Karst.) L), in view of the assumption that foliage along the shoot will influence the hydraulic architecture. Applying the zero-order assumption of the WBE model (West et al. 1999) to within-shoot structure, this would mean that the number of conduits would increase in proportion to the cumulative foliage area from shoot tip to base. We will seek answers to the following novel research questions:

1) How does shoot structure relate to water transport when accounting for needle positioning along the shoot?

2) How does shoot hydraulic conductance, i.e. water supply to the shoot, scale with shoot size, and does it enhance apical dominance?

3) How does shoot structure relate to theoretical and empirical scaling rules established in previous literature?

To answer these questions, we will first develop a model of the anatomical structure in the shoots, then apply this to data to establish scaling exponents and other parameters, and apply the results to simulate the water potential within individual shoots of different sizes at the end of the water conducting pathway in a tree. Finally, we discuss our results in comparison with previous studies on shoot and tree scaling relations and their implications on water potential.

Material and methods

Modelling scaling relations and water potential gradient

Basic relationships. Consider the water flux, $J(x)$, within a shoot axis as a function of distance from the apex, x. The flux density to the foliage at x corresponds to transpiration from the foliage, $T(x)$, and is created by leaf area per unit length at x, $A_L(x)$, and its transpiration flux per unit foliage area, $E(x)$

$$\frac{dJ}{dx} = T(x) = A_L(x)\, E(x) \qquad (1)$$

In the allometric scaling models (West et al. 1999, Savage et al. 2010) all foliage is attached to the end of the shoot, such that $T(x) = 0$ along the shoot and $J(x)$ is constant. Here, we shall first assume that both $A_L(x)$ and $E(x)$ are constant along the shoot. Under this assumption we have

$$J(x) = Tx \tag{2}$$

On the other hand, the flux at x depends on sapwood area (A_S) at x, shoot conductivity per sapwood area (K_S) at x , and the gradient of the water potential, Ψ:

$$J(x) = K_S(x)A_S(x)\frac{d\Psi}{dx} \tag{3}$$

This allows us to determine the water potential gradient along the shoot:

$$\frac{d\Psi}{dx} = \frac{J(x)}{K_S(x)A_S(x)} \tag{4}$$

indicating its dependence on shoot conductive properties and the water flux which is the integral of transpiration.

Shoot shape and hydraulic properties. Denote by ξ the relative distance from the apex, i.e. $x = L\xi$ where L is shoot length. Following the general formulations in hydraulic scaling models, we consider the following scaling relationships (see Table 1 for the symbols used):

SR1) Shoot basal diameter, $D(L)$, scales with shoot length, while the relative diameter within the shoot scales with the relative distance from shoot apex, ξ:

$$D(x) = D(\xi L) = \alpha_D L^u \xi^v \tag{5}$$

Here, u and v are scaling exponents and α_D is a proportionality coefficient. This formulation allows us to consider the possibility of different scaling between and within shoots. E.g., $u = 3/2$ and $v = 0$ represent cylindrical shoots following the quarter-power allometric scaling (West et al. 1999, Savage et al. 2010). On the other hand, $u = v$ would imply that that all shoots are identical in size and shape near the apex but may differ in total length and basal diameter (Figure 1).

SR2) Conduit hydraulic diameter scales with shoot diameter:

$$d_H(x) = \alpha_H D(x)^z \qquad (6)$$

where z is a scaling exponent and α_H is an empirical constant. This trend has been found in many earlier studies (e.g. Savage et al. 2010, Olson and Rosell 2013, Jyske and Hölttä 2015). The condition $u = v$ in SR1 would imply that conduit diameter within the shoot scales with the *absolute* distance from shoot apex, whereas if $u \neq v$ it would scale with *relative* distance ($d_H(x) \propto L^{uz}\xi^{vz}$).

SR3) According to the Poiseulle equation sapwood conductivity scales as $K_S(x) \propto n(x)d_H(x)^4$, where $n(x)$ is the density of tracheids in sapwood. The latter has been assumed in scaling models to be either inversely proportional to tracheid area (Sperry et al. 2008, Savage et al. 2010), or constant (West et al. 1999). This yields for hydraulic conductivity

$$K_S(x) = a_{KH} d_H(x)^w = a_{KD} D(x)^{wz} \qquad (7)$$

where a_{KH} and a_{KD} are empirical constants and $4 \geq w \geq 2$ (assuming that that pit conductance scales linearly with lumen conductance) (Lazzarin et al. 2016).

SR4) Shoot sapwood area scales with shoot diameter

$$A_S(x) = a_S D(x)^{2-s} \qquad (8)$$

where a_S is an empirical constant and the exponent s accounts for the scaling of the share of sapwood with shoot diameter (West et al. 1999, Savage et al. 2010).

SR5) Total foliage area of the shoot scales with shoot length:

$$A_L = a_L L^{\gamma} \quad (9)$$

where a_L is an empirical constant and γ is the scaling exponent (West et al. 1999, Savage et al. 2010).

Implications of shoot size and shape on water potential gradient. Inserting the scaling relationships SR1-SR5 and Eqn (2) into Eqn (4) yields

$$\frac{d\Psi}{dx} = \frac{a_L L^{\gamma}\, E(\frac{x}{L})^b \times 10^{-4}}{a_{KD} D(x)^{wz} a_S D(x)^{2-s} \times 10^{-6}} \quad (10)$$

where we have introduced the exponent b to allow us to consider different distributions of transpiration along the shoot; particularly, $b = 0$ for the assumption that all foliage is attached to the end of the shoot and $b = 1$ if transpiration is evenly distributed along the shoot (Supplementary material S1) (see Table 1 for units). Because Eqn (5) splits the dependence of $D(x)$ on x into two components, shoot length L and distance from the apex, ξ, it is convenient to express the water potential gradient in terms of ξ instead x:

$$\frac{d\Psi}{d\xi} = \frac{d\Psi}{dx}\frac{dx}{d\xi} = L \times 10^{-3} \times \frac{a_L L^{\gamma}\, E\xi^b \times 10^{-4}}{a_{KD} D(L\xi)^{wz} a_S D(L\xi)^{2-s} \times 10^{-6}} \quad (11)$$

Inserting Eqn (5) and rearranging Eqn (11) (S1) yields

$$\frac{d\Psi}{d\xi} = K(L) \times \xi^{b-v(wz+2-s)} \quad (12a)$$

where

$$K(L) = \frac{E a_L \times 10^{-1}}{a_S a_{KD} {a_D}^{wz+2-s}} L^p \qquad (12b)$$

and

$$p = \gamma + 1 - u(wz + 2 - s) \qquad (12c)$$

Now the water potential gradient can be integrated over the shoot, which yields (S1):

$$\Psi(\xi) = \Psi(1) - \frac{K(L)}{q}(1 - \xi^q) \quad \text{if} \quad q \neq -1$$
$$\Psi(\xi) = \Psi(1) + K(L)\ln(\xi), \quad \text{if} \quad q = -1 \qquad (13a)$$

where

$$q = 1 + b - v(wz + 2 - s) \qquad (13b)$$

This shows that the water potential along the shoot depends on the water potential at shoot base $\Psi(1)$, on shoot size and scaling (shape) through $K(L)$ and q, and on the distance from the apex through ξ.

We quantified the shoot water potential of Eqn (13) using scaling parameters (Eqns 5-9) obtained from measurements on 1st year Scots pine and Norway spruce shoots (see below). These were combined with our previous estimates of water potential at the base of the current year shoot ($\Psi(1)$) and foliar transpiration rate E. These allowed us to study the quantitative dependence of shoot water potential on shoot structure and size.

Measurements

We sampled current-year shoots of planted saplings of *Pinus sylvestris* and *Picea abies* and those of naturally regenerated under-storey saplings of *Picea abies* in August 2014 in southwest Finland, Hyytiälä, Juupajoki (61°50'N, 24°18 E). The understorey saplings were included to represent a wider range of shoot sizes from the same branching level. The plantations were established in 2005 and the planted saplings were about 2m and

the under-storey saplings about 1 m tall. Five non-leader shoots were collected from five saplings in planted pine, planted spruce and under-storey spruce, one from each whorl of branches born in the latest 5 years (Table 2, Table S3.1). The shoots were taken to the laboratory and measured for length and basal diameter under bark and dried for foliage mass measurement (105 °C, 24 h). All-sided specific leaf area (SLA) was estimated from five sample needles per shoot following Grönlund et al. (2016). Foliage area was calculated by multiplying SLA and foliage dry mass.

Three of the planted saplings of each species and two of the naturally regenerated spruce saplings were selected as a sub-sample for analysing the shoot shape and wood anatomical structure. Two shoots, one from the 1st and one from the 4th whorl of the planted saplings and one shoot from the 3rd whorl of the natural spruce saplings were selected for this analysis (Table 2, Table S3.1). Two samples of each shoot were taken at 20% and 80% distance from the base for measuring shoot diameter and distance from the apex, tracheid area, tracheid density and tracheid diameter and percentage of non-conducting pith of the sample. This allowed us to analyse the external shape of the shoots (Figure 1) and at the same time to estimate a rule for the postulated widening of conduits with shoot diameter and / or distance from shoot tip.

An additional sampling was carried out in September 2017 in the same sapling stands (height now 2.5-3 m) to evaluate the distribution of needle mass over shoot length. Three saplings of pine and spruce were selected and 5 current-year shoots were sampled from each tree, two from the top whorl and three from either 3rd or 4th whorl down (Table 2, Table S3.1). The shoots were taken to the laboratory, cut into five segments of equal length and dried (105 ^{o}C 24 h) for needle dry mass measurement.

For measuring tracheid area and density, a 1 cm piece was cut at the two sample locations of each sample shoot and stored in the freezer. Microscopic sections were prepared from these pieces using ice microtome Leica CM 3050 S (Leica Biosystems, Wetzlar, Germany). The ice microtome freezes the piece of wood on the adapter. Water is made to drip on to the sample in cold environment until fully frozen. The adapter is then

mounted on the microtome and the desired thickness of the sections (here 20 µm) is set. A total of 8-10 sections were cut and transferred on object glass, then coloured with Safranin and finally dried by using an alcohol series . Preparations were made permanent using Canadian balsam. After a few days of drying, all the sections were checked under a microscope and the best one from each sample was selected for measurements.

The sections were photographed with an Olympus ALTRA 20 colour camera attached to an Olympus CX 31 microscope (Olympus Optical Co., Tokyo, Japan). One photo was taken of the whole section with ×40 magnification. The section was then divided into four 90° sectors, and one sample image with ×400 magnification was taken of each sector (Figure 2). Sample images were taken of the earlywood part of the sample and covered ~5% of the sector area. Average tracheid density and area values were measured manually from these sample images. Every tracheid of every image was digitized to obtain the lumen area and the number of tracheids in the picture frame. We measured 3587 tracheids in total, averaging approximately 32 tracheids per sample. The cross section values of density and area were calculated as averages over these four sample images. All the calculations were made using the image analysis program ImagePro (Media Cybernetics, Inc., Rockville, MD, USA).

The sapwood-area specific hydraulic conductivity, K_S (m^2 Pa^{-1} s^{-1}), was estimated from the sample measurements of tracheid area and sample area (Tyree & Ewers 1991):

$$K_S = \frac{1}{4}\sum_{j=1}^{4}\frac{1}{A_j}\frac{\sum_i A_{ij}^2/\pi}{8 \times 0.001} \qquad (14)$$

where the first sum is over the four samples (j) from the sectors. A_j (m^2) is the area of sample j, A_{ij} (m^2) is the lumen area of the i'th tracheid of sample j, and 0.001 is the dynamic viscosity of water ($\mathrm{Pa} \times \mathrm{s}$). All tracheids were assumed conducting.

Lumen diameter d_i was calculated from lumen area with the assumption of circular lumen cross-section. This was taken as the hydraulic diameter, and it is approximately directly proportional to the hydraulic diameter defined by Mencuccini et al. (1997) when the ratio of longer to shorter side of the lumen is in the range $[1/3,3]$. The weighted average, d_H , of the hydraulic diameter was calculated as

$$d_H = \frac{\sum d_i^5}{\sum d_i^4} \qquad (15)$$

which weights the hydraulic diameters according to hydraulic conductance (Sperry et al., 1994). This averaging is standard when analysing hydraulic conductivity (Kolb and Sperry 1999, Jyske and Hölttä 2015).

Methods

Statistical tests. The scaling exponents and coefficients of proportionality were estimated by linear regression of the logarithmic transformation of the equations. The significance of the regressions was assessed using the F test, requiring $p < 0.05$. Differences between groups (tip and base measurements, species, and species with spruce in light and shade subgroups) were assessed by applying the t test on the equality of the regression coefficients ($p < 0.05$). The equality of means of variables between groups was assessed using ANOVA. All statistical analyses were made with R software (R Development Core Team 2015).

Calculations and simulation. We used the analytical solution (13) for calculating the water potential in shoots with measured and hypothetical properties (S1). These included a comparison of cylindrical and paraboloid shapes and foliage attached to the end or evenly along the shoot. We considered cylindrical shoots with the same basal diameter and with the same woody volume as paraboloid shoots. Conduit diameter was determined on the basis of the external basal diameter in the hypothetical (cylindrical and paraboloid) shoots, i.e., no conduit widening was included in the calculations for these hypothetical shapes. When making the

calculations for shoots of the measured shape, we also included measured conduit widening. The comparison of shoot shapes was done using a standard shoot length of 10 cm.

In addition, we analysed cases with non-even distribution of transpiration by solving Eqn (4) numerically (Supplementary material S2). Here our objective was to analyse cases where transpiration is checked by uneven distribution of either foliage mass or stomatal opening.

In the even-distribution cases the default foliage-specific transpiration was set to $E = 0.06 \times 10^{-6}$ $\mathrm{m^3\ m^{-2}\ s^{-1}}$ which represents unshaded foliage of pine seedlings around noon (our own unpublished data, see also Vanderklein et al. 2007). E was modified linearly in the cases with variable transpiration rates. In all cases, we assumed that the shoot was attached to woody pathway with total conductance K_{tot}, which in turn was attached to the soil at water potential $\Psi_{soil} = 0$ MPa. The total conductance was estimated on the basis of our unpublished data on pine seedlings where the water potential at the end of the pathway was about -0.8 MPa, so K_{tot} was set to 7.5×10^{-14} m $\mathrm{Pa^{-1}\ s^{-1}}$ and is also in line with other similar measurements (Vanderklein et al. 2007). The sapwood specific conductivities estimated from anatomical data in this study were multiplied by a factor 0.25 because this was approximately the ratio between measured and calculated hydraulic conductivity (which, like in this study, was based on lumen area not accounting for pit size) from similar shoots in the study by Grönlund et al. (2016).

Results

Shoot shape and hydraulic properties

The basal diameter of the shoots $D(L)$ scaled with shoot length L with scaling exponent u not statistically different from 1 when all groups (pine, spruce in light and spruce in shade) were assumed to have the same exponent with different coefficients ($t = 0.813, p = 0.419$) (Table 3, Figure 3a). Linear models fitted

through the origin differed between pine and spruce but not between the two spruce populations ($p = 0.585$). The basal diameter of pine shoots was larger than that of spruce shoots for the same shoot length (Table 3, Figure 3a), as was the foliage area (Figure 3b).

The diameter of the shoots at 20% distance from the tip was on average 72±4.7 % of the diameter at 80% distance from the tip and did not vary significantly between pine, spruce in light and spruce in shade ($F = 0.237, p = 0.793$). The mean scaling exponent v (scaling of shoot diameter with relative length, Eqn 5) in the data set was found to be $v = 0.237$ (Table 3, Supplementary material S3). A t-test of the exponents of spruce in shade and pine against spruce in light showed no differences ($t = 0.94203$ and $t = 0.44565$, respectively). Similar analyses for conduit diameter showed that the ratio of apex to base conduit diameter was on average 0.899 ± 0.0575, with the largest value in open-grown spruce (0.936 ± 0.0395), lowest in understorey spruce (0.847 ± 0.0198) and pine with an intermediate value (0.880 ± 0.0618), but the differences were not statistically significant ($F = 3.184, p = 0.0811$) (S3).

Conduit hydraulic diameter (d_H) scaled with distance from the branch tip (Table 3, Figure 3c) and shoot diameter (Table 3, Figure 3d). However, the scaling between conduit diameter and the distance from the apex varied between the samples taken at 20% and 80% distance from the apex ($t = 5.406, p < 0.001$) (Figure 3c). The calculated sapwood hydraulic conductivity K_S of the shoot (Eqn 14) scaled with the hydraulic diameter with exponent $w = 2.43$ (Table 3, Figure 3e) and with shoot diameter with exponent $wz = 0.745$ (Table 3, Figure 3f), and these relationships did not differ statistically significantly between shoot positions or species. The density of conduits was closely related to the inverse of the square root of shoot area (scaling exponent -0.477 with respect to diameter) (S3). The scaling of conduit density with hydraulic diameter is hence $-\frac{0.477}{z} = -1.55$.

The share of pith of shoot cross-sectional area was larger in spruce (45.0 ±5.95 %) than pine (24.3 ± 5.35 %) ($F = 34.3, p < 0.001$). The average in both species was smaller in the sample closer to the apex, but these differences

were not statistically significant ($F = 0.672,\ p = 0.420$). However, the share of pith in total shoot area increased with increasing diameter in both species. This increase was statistically significant in spruce ($F = 9.153, p = 0.009$) but not in pine, and the exponent s (ratio of conducting to non-conducting area vs. external diameter) vanishes for pine but takes the value $s = 0.21$ for spruce (Table 3, Figure 3f).

The needle mass distribution was declining from shoot apex to base in pine and the trend was significant with $R^2 = 0.603$ $(t = -10.53, p < 0.001)$. In spruce there was no trend with distance from the apex ($t = 1.203$, $p = 0.233$) (Figure 4).

Implications on shoot water potential

Impact of shoot shape on water potential gradient. A comparison of 10-cm pine shoots with different assumptions on structure showed that shoot properties and geometry have a significant influence on shoot water potential (Figure 5). Cylindrical shoots with evenly distributed foliage and the same basal diameter as the paraboloid (and measured) shoots showed the most shallow water potential gradient, while in the paraboloid shoots with foliage attached to the end the water potential at the tip approached $-\infty$ (S1). The paraboloid shoot with evenly distributed foliage and the same basal diameter as the cylindrical shoot with foliage at the end manifested identical water potential gradients (Figure 5a). When the volume of the cylindrical shoot was reduced to that of the paraboloid shoot, its water potential reduced considerably (Figure 5a). Shoots with measured properties were intermediate between cylinders and paraboloids with evenly distributed foliage, whereas shoots with measured structure but foliage attached to the end showed a rapid decline in water potential towards the apex (Figure 5b). The gradient was steeper in pine than spruce, due to its smaller foliage area for a given shoot length (see Figure 3b).

Impact of shoot size. As predicted by Eqn (13) applied with the measured parameter values, the water potential loss in the shoot increased with decreasing shoot size under the same evaporative demand (i.e., transpiration per unit foliage area, E), and more so in pine than spruce (Figure 6a). Reducing E would reduce the water potential loss over the shoot, such that for each length, a respective E could be determined that would lead to the same loss of water potential in all shoots (Figure 6b). For example, a 100 mm shoot could only transpire at a foliage-specific rate of about a third of that of a 500 mm shoot to maintain the same loss of water potential as the longer shoot. This relationship was very similar in pine and spruce (Figure 6b).

Impact of uneven distribution of transpiration. Using the measured foliage distribution for pine instead of the even distribution assumed above had only a minor effect on the water potential loss, increasing it somewhat because of the increasing foliage density towards the apex (Figure 7). On the other hand, the assumption of a linear decrease of transpiration from base to apex reduced the water potential loss considerably, even if the total transpiration of the shoot was held constant. An even bigger reduction in the water potential loss was obtained under the assumption that total transpiration was halved (Figure 7).

Discussion

We found that current shoots in pine and spruce showed regularity of shape and shared scaling rules (Table 2). Their external shape could be described using two scaling exponents, one relating shoot length to its basal diameter (u), the other characterising the relative widening of the shoot from apex to base (v). Shoot length and diameter were linearly related with $u = 1$ (Figure 3, Table 2) which corresponds to geometric similarity (Niklas 1995), instead of the elastic similarity ($u = 2/3$) assumed by the quarter-power scaling model (West et al. 1999, Savage et al. 2010), and is close to the value $u = 0.97$ found previously for entire branches of Scots pine (Hölttä et al. 2013). The external shape of the shoots ($v = 0.237$) was intermediate between cylinder ($v = 0$) and paraboloid ($v = 0.5$) (Figures 1 and S4.1). Shape stability is indicative of strong selective pressures.

Paraboloid shape represents the pipe model at the shoot level (i.e., that conducting area at a point along the shoot axis is proportional to cumulative foliage area from shoot tip to that point) and leads to identical water potential gradient with the cylindrical shape where foliage is at the apex (assuming no conduit widening) (Figure 5). At the same time, it would only require half of the woody growth investment compared with the cylinder. On the other hand, the cylinder could be taken to represent a growth pattern that efficiently prepares for next year's growth, providing a suitable base for the new shoot to attach upon. Shoot shape therefore seems to be a compromise between effective use of photosynthates for current year requirements of water transport, and for future need of support and conductance.

We also found regular within-shoot scaling of conduit diameter and hydraulic conductivity with shoot diameter. Within-shoot conduit scaling has been ignored in scaling theories that theoretically describe shoots as cylinders with constant shoot diameter and conduit diameter (West et al. 1999, Savage et al. 2010). The within-shoot scaling was very close to the inter-segment scaling predicted by Savage et al. (2010) and also close to observed values of inter-segment scaling of hydraulic diameter and other derived variables (Savage et al. 2010, Table S4.1). Particularly, our relationship between shoot diameter and conduit hydraulic diameter was almost identical with that found by Jyske and Hölttä (2015) close to branch tips in Norway spruce (Figure 3d, Table S4.1), although the conduits further from the tip (in older branch parts) were rather constant in diameter along the entire pathway. In the light of this study, this could be related to the presence of foliage along the water transport pathway, whereas further along the branches, foliage has already been shed.

We estimated that less than 5-10% of the resistance to water flow (i.e. water potential drop) was confined to the current shoot in spruce and pine seedlings (Figure 5). Although this is more than the relative share of the shoots in the length of the hydraulic pathway, it is less than suggested in previous literature (Tyree & Evers 1991). Accounting for the needle distribution along the shoots led to considerably lower water potential losses along the shoot than with foliage located at the apex (Figure 5). The difference was particularly large if the observed shoot properties were assumed with foliage at the apex, but even the cylindrical shoots with foliage

at the end gave a larger water potential loss than the shoots with measured structure. This suggests that placing the foliage at the end of the water transport pathway, as is done in the hydraulic scaling models (West et al. 1999, Savage et al. 2010, Sperry et al. 2012) considerably overestimates the water potential loss over the transport pathway. The total overestimation may be even larger in evergreen conifers as foliage is also present in older branch segments, the lifetime of foliage varying from 3 to 12 years in pine and spruce in Finland (Tupek et al. 2015) and even up to 45 years in *Pinus longaeva* (Ewers and Schmid 1981). Furthermore, our simulation of the variable transpiration rate along the shoot demonstrated that shoots with distributed foliage could further reduce their water potential loss by partial stomatal control. If stomata were closed near the apex, the overall water potential loss would be reduced, even if the rest of the foliage were transpiring and hence photosynthesising at full capacity (Figure 7). Ignoring this in models could lead to overestimation of hydraulic effects on leaf gas exchange.

According to our results, larger shoots show a lower loss of water potential over shoot length than shorter shoots (Figure 6). This is mainly because larger shoots in the data had a higher xylem-area-specific conductivity than smaller shoots, due to larger hydraulic diameter of conduits (Figure 3d). Here we assumed that transpiration was constant per unit foliage area. This renders foliage-specific whole-shoot conductance, defined as foliage-specific flux divided by water potential loss across the whole shoot (e.g. Yang and Tyree 1993), larger in larger shoots. This is opposite to findings concerning whole trees or tree segments that consist of multiple age cohorts of shoots, where foliage-specific whole segment conductance has been found to decrease with segment size (Table S4.1, Yang and Tyree 1993, Mencuccini and Grace 1996, Mencuccini 2002). It is this inter-level scaling that is also described by the hydraulic scaling models whereas units at one level are always of the same size in the theoretical models. Our results suggest that size variation between current-year shoots influences the hydraulic relationships in the whole crown.

The size variation between new shoots can be caused by genetically-determined apical dominance or environmental conditions (Oliver and Larson 1996, Nikinmaa et al. 2003). In a new whorl of shoots, the apical

shoot is usually bigger than the lateral shoots, and the implied higher conductivity and whole-shoot conductance would further favour the future growth of the apex relative to the laterals. If lateral branches as a whole have lower conductance than the stem (Zimmermann 1983, Tyree et al. 1991), this could further emphasize the apical dominance. In crowns inside the canopy the light environment and evaporative demand usually decline downwards in the tree crown, where shoot size is also reduced (e.g. Grönlund et al. 2016). Our simulations indicated that although the structure of smaller shoots would lead to steeper water potential gradients than in bigger shoots under the same evaporative demand, the loss could be checked with reduced transpiration rates. In our results a 50% reduction of the foliage-specific transpiration rate from 50 to 20 cm shoots led to the same water potential loss from base to apex (Figure 6). This is an indication that bigger shoots are better adapted than small shoots to high light conditions.

The height growth of trees reaches a peak at a young age, in pine and spruce at our measurement site around the age of 20 years, after which the length of both the leader and other shoots is decreasing. In old trees new shoots, i.e., annual growth of the branches can be just a few centimeters. Our results suggest that this could bring about a considerable increase in tree-level hydraulic resistance (Figure 6) and could significantly contribute to the measured decline in whole-tree conductance with tree age (or size) (Ryan et al. 2000), in addition to the increased resistance of the hydraulic pathway from root to the base of the current-year shoot (Mencuccini 2002, Savage et al. 2010). This conclusion assumes that the relationship between shoot diameter and conduit hydraulic diameter can be generalised to trees of all ages. While more measurements are required to test this proposition, it is corroborated by a comparison with our previous study where we measured shoots from 30-year-old Scots pine trees (height 10-15 m) and obtained a very similar relationship between hydraulic diameter and shoot basal diameter (Grönlund et al. 2016). On the other hand, Prendin et al. (2018) found that hydraulic conductivity in the stem at 10 cm from the apex showed a weak but statistically significant increase with tree height in Norway spruce trees with annual growth rates ≤ 10 cm, suggesting that subsequent secondary growth could compensate for the low conductivity in the shortest shoots.

Many studies have analysed the scaling between hydraulic diameter and distance from the apex along stems and branches (Mencuccini et al. 2007, Petit et al. 2008, Jyske and Hölttä 2014, Table S4.1). From the point of view of the scaling theory this is problematic because, theoretically, there is no widening of external nor internal (conduit) diameter within a branch segment, but there should be widening between segments. In empirical scaling studies the assumption of no widening within segments has usually been relaxed, but a consistent scaling relationship between conduit diameter and distance from the apex would have to assume that the two scaling exponents are the same, i.e., $u = v$. If this was not the case, we should expect the scaling with distance from the apex to be dependent on the relative distance within the segment as well, similarly to our results for the new shoots (Figure 3c). This is probably why the observed scaling with distance from the apex has resulted in a larger variability of exponents than scaling with diameter (Jyske and Hölttä 2015), and the distance-based scaling exponent near the apex has been found either smaller (Petit et al. 2008) or larger (Mencuccini et al. 2007) than that over entire stems or branches.

Quite independently of allometric scaling models, it has been argued that conduit diameter should scale with distance from the apex in order to allow for balanced water transport, and this proposition has gained empirical support in large, mainly angiosperm multi-species data sets (Olson and Rosell 2013, Olson et al. 2014, Rosell et al. 2017). Our study is to our knowledge the first one that has focused on the variability of conduit size at a much finer scale: within-shoot variation in current-year shoots of two boreal conifers. At least at this scale and for these two conifer species the postulated general relationship between absolute distance from apex and conduit diameter failed to hold true. Instead, we found a tight relationship between shoot diameter and conduit diameter, whereas neither of these scaled with absolute distance from shoot apex. While the possible biological and physiological reasons for this discrepancy remain unclear, we have suggested above that the rate of widening of the shoot and its conductive area could be related to a trade-off between optimal hydraulics in the current year and optimal shoot structure for supporting new shoots in subsequent years.

Our whole-tree water potential calculations were simplified and the results therefore are largely qualitative. The foliage-specific transpiration rate used here represents a midday rate during the summer at the site of measurements and hence the results relate to situations of high evaporative demand (unpublished laboratory measurements). However, the relationship between shoot and whole-tree conductance is independent of this assumption. Secondly, we assumed that the real conductivity was proportional to theoretical, calculated conductivity with a coefficient obtained from a previous study (Grönlund et al. 2016), rather than modelling any details such as the size of torus–margo pits in the tracheids (Hacke et al. 2004). Thirdly, we assumed that the water potential at the base of the shoot was independent of shoot size (or branch order). These assumptions could be relaxed in a more detailed model analysis, such as that conducted by Sperry et al. (2012), to further investigate the significance of current shoot structure on whole-tree hydraulic properties and scaling relationships.

Conclusions

Consistent with hydraulic theory, we found that conduit and shoot diameters were inherently related. Shoot shape was intermediate between cylindrical and paraboloid, which was interpreted as a compromise between current water transport and investment in future growth. Within-shoot conduit diameter scaled with relative, not absolute, distance from the apex. Its scaling with shoot diameter was independent of species and quantitatively close to previous findings in stem wood near the apex and in branch and stem segments in conifers. Consequently, shoot hydraulic conductivity also manifested an allometric relationship with both shoot diameter and conduit diameter. Importantly, larger shoots had higher hydraulic conductance thus driving

future growth to them and enhancing apical dominance. Current-year shoots represented a fair part of water potential loss in the tree. The results suggest that ignoring the foliage distribution along the hydraulic pathway and the size variability of shoots tends to overestimate water potential loss in branches and therefore to overestimate related water stress effects. On the other hand, ignoring the age-related variability of shoot size could overestimate shoot conductance in old trees.

Conflict of interest: none declared

Funding: Annikki Mäkelä and Pauliina Schiestl-Aalto were supported by the Knut and Alice Wallenberg Foundation (#2015.0047).

Authors' contributions: AM and TH developed the original concept, LG conducted the shoot hydraulic structure measurements and initial data processing and analysis, PSA conducted the foliage distribution measurements, AM analysed the data and was responsible for writing the manuscript, AM and TH did the modelling and simulations, TK commented on the study and manuscript at various stages, all commented on the manuscript during the writing process

References

Brodribb, T. J. 2009. Xylem hydraulic physiology: the functional backbone of terrestrial plant productivity. *Plant Science*, *177*(4), 245-251

Cochard H., 1992. Vulnerability of several conifers to air embolism. *Tree Physiology* 11 (1992) 73–83

Duursma R.A., Kolari P., Perämäki M., Nikinmaa E., Hari P., Delzon S., Loustau D., Ilvesniemi H., Pumpanen J., Mäkelä A. 2008. Predicting the decline in daily maximum transpiration rate of two pine stands during drought based on constant minimum leaf water potential and plant hydraulic conductance. *Tree Physiology* 28, 265-276.

Duursma, R.A., Mäkelä, A., Reid, D.E.B., Jokela, E.J., Porté, A., Roberts, S.D. 2010. Self-shading affects allometric scaling in trees. *Functional Ecology* 24:723-730.

Ewers, F. W., and R. Schmid. 1981. Longevity of needle fascicles of Pinus longaeva (Bristlecone pine) and other North American pines. *Oecologia* 51:107–115.Grönlund L., Hölttä T., Mäkelä A. 2016. Branch age and light conditions determine leaf-area specific conductivity in current shoots of Scots pine. *Tree Physiology* 36:994-1006

Hacke, U. G., Sperry, J. S., & Pittermann, J. (2004). Analysis of circular bordered pit function II. Gymnosperm tracheids with torus-margo pit membranes. *American Journal of Botany*, *91*(3), 386-400.

Hölttä, T., Kurppa, M., & Nikinmaa, E. 2013. Scaling of xylem and phloem transport capacity and resource usage with tree size. *Frontiers in plant science*, *4*, 496.

Huber B 1928. Weitere quantitative Untersuchungen über das Wasserlitungssystem der Pflanzen. Jb Wiss Bot 67: 877-959.

Jyske T, Hölttä T 2015. Comparison of phloem and xylem hydraulic architecture in *Picea abies* stems. New Phytologist 205:102-115. doi: 10.1111/nph.12973

Kozlowski T.T., Kramer P.J., Pallardy S.G. 1991. The physiological Ecology of Woody Plants. Academic Press, Inc. San Diego, California 92101. 657 pp.

Lintunen A, Kalliokoski T 2010. The effect of tree architecture on conduit diameter and frequency from small distal roots to branch tips in *Betula pendula*, *Picea abies* and *Pinus sylvestris.* Tree Physiology 30: 1433-1447.

McCulloh, K. A., Sperry, J. S., & Adler, F. R. 2003. Water transport in plants obeys Murray's law. *Nature*, *421*(6926), 939.

Mencuccini M 2002. Hydraulic constraints in the functional scaling of trees. Tree Physiology 22, 553–565.

Mencuccini M, Grace J. 1996. Developmental patterns of aboveground xylem conductance in a Scots pine (*Pinus sylvestris* L.) age sequence. Plant Cell Environ. 19:939–948.

Mencuccini M, Grace J, Fioravanti M. 1997. Biomechanical and hydraulic determinants of tree structure in Scots pine: anatomical characteristics. *Tree Physiology* 17: 105–113.

Mencuccini M, Hölttä T, Petit G, Magnani F 2007. Sanio's laws revisited. Size-dependent changes in the xylem architecture of trees. Ecol Lett 10:1084–1093.

Nikinmaa, E., Messier, C., Sievänen, R., Perttunen, J. & Lehtonen, M. 2003. Shoot growth and crown development: effect of crown position in three-dimensional simulations. Tree Physiology 23: 129-136.

Niklas, K. J. 1995. Size-dependent allometry of tree height, diameter and trunk-taper. *Annals of botany*, *75*(3), 217-227.

Oliver CH, Larson BC 1996. Forest stand dynamics. Update edition. John Wiley and Sons, Inc. New York. 520 pp.

Olson, M. E., & Rosell, J. A. 2013. Vessel diameter–stem diameter scaling across woody angiosperms and the ecological causes of xylem vessel diameter variation. *New Phytologist*, *197*(4), 1204-1213.

Olson, M. E., T. Anfodillo, J. A. Rosell, G. Petit, A. Crivellaro, S. Isnard, C. León-Gómez, L. O. Alvarado-Cárdenas, and M. Castorena. 2014. Universal hydraulics of the flowering plants: vessel diameter scales with stem length across angiosperm lineages, habits and climates. Ecology Letters 17:988–997.

Petit G, Anfodillo T, Mencuccini M. 2008. Tapering of xylem conduits and hydraulic limitations in sycamore (*Acer pseudoplatanus*) trees. *New Phytologist* **177**: 653–664. **doi**: 10.1111/j.1469-8137.2007.02291.x

Rosell, J. A., M. E. Olson, and T. Anfodillo. 2017. Scaling of xylem vessel diameter with plant size: causes, predictions, and outstanding questions. Current Forestry Reports 3:46–59.

Ryan M.G:, Bond B.J., Law B.E., Hubbard R.M., Woodruff D., Cienciala E., Kucera J. 2000. Transpiration and whole-tree conductance in ponderosa pine trees of different heights. Oecologia 124:553–560.

Savage VM, Bentley LP, Enquist BJ, Sperry JS, Smith DD, Reich PB, von Allmen EI 2010. Hydraulic trade-offs and space filling enable better predictions of vascular structure and function in plants. PNAS 107(52):22722-22727. doi.org/10.1073/pnas.1012194108

Kolb, K.J. and Sperry, J.S. 1999. Transport constraints on water use by the Great Basin shrub, Artemisia tridentata. Plant Cell Environ. 80: 2372–2384.

Sperry JS, Nicholas KL, Sullivan JEM, Eastlack SE. 1994. Xylem embolism in ring porous, diffuse porous, and coniferous trees of northern Utah and interior Alaska. *Ecology* 75: 1736–1752.

Sperry, J. S., Meinzer, F. C., & McCulloh, K. A. 2008. Safety and efficiency conflicts in hydraulic architecture: scaling from tissues to trees. *Plant, Cell & Environment*, *31*(5), 632-645.

Sperry JS, Smith DD, Savage VM, Enquist BJ, McCulloh KA, Reich PB, Bentley LP, von Allmen EI 2012. A species-level model for metabolic scaling in trees I. Exploring boundaries to scaling space within and across species. Functional Ecology 2012, 26, 1054–1065

Ťupek B., Mäkipää R., Heikkinen J., Peltoniemi M., Ukonmaanaho L., Hokkanen T., Nöjd P., Nevalainen S., Lindgren M. & Lehtonen A. 2015. Foliar turnover rates in Finland — comparing estimates from needle-cohort and litterfall-biomass methods. Boreal Environment Research 20: 283–304.

Tyree M.T., Ewers F.W. 1991. The hydraulic architecture of trees and other woody plants. New Phytologist 119:345–360.

Tyree M.T., Snyderman D.A., Wilmot T.R., Machado J.-L. 1991. Water Relations and Hydraulic Architecture of a Tropical Tree (Schefflera morototoni). Data, Models, and a Comparison with Two Temperate Species (*Acer saccharum* and *Thuja occidentalis*). Plant Physiology 96:1105-1113.

Vanderklein D., Martínez-Vilalta J., Lee S., Mencuccini M. 2007. Plant size, not age, regulates growth and gas exchange in grafted Scots pine trees. Tree Physiology 27: 71-79.

West G.B., Brown J.H., Enquist B.J. 1999. A general model for the structure and allometry of plant vascular systems. Nature 400:664–667.

Yang, S., Tyree, M. T. (1993). Hydraulic resistance in Acer saccharum shoots and its influence on leaf water potential and transpiration. *Tree Physiology*, *12*(3), 231-242.

Zimmermann M.H. 1983. Xylem structure and the ascent of sap. Springer-Verlag. Berlin, Heidelberg, New York, Tokyo. 143 pp.

Table 1. Symbols, their definitions and units used in the scaling analysis.

Symbol	Meaning	Units used in analysis
x	Distance from apex along shoot	mm
L	Shoot length	mm
$\xi = x/L$	Relative distance from apex along shoot	unitless
$D(x)$	Shoot diameter at distance x	mm
A_L	Total shoot leaf area	cm^2
$A_S(x)$	Sapwood area at distance x	mm^2
$K_S(x)$	Sapwood specific hydraulic conductivity at x	m Pa^{-1} s^{-1}
$J(x)$	Water flux at distance x	$m^3 s^{-1}$
$\Psi(x)$	Water potential at distance x	Pa
$d_H(x)$	Hydraulic diameter at distance x	µm
K_{tot}	Hydraulic conductance from soil to shoot base	7.5×10^{-14} m Pa^{-1} s^{-1}
E	Foliage-area specific transpiration	0.06×10^{-6} m^3 m^{-2} s^{-1}
Ψ_{soil}	Soil water potential	0 Pa

Table 2. Study material. "Branch age" refers to the age of parent branches from which the current-year, non-leader shoots were collected. The within-shoot properties were measured at 20% and 80% length of each shoot.

	Whole-shoot allometry (2014 whole set)			**Within-shoot properties** (2014 subset)			**Foliage distribution** (2017 added data)		
Species group	*Nr of trees*	*Nr of shoots*	*Branch age*	*Nr of trees*	*Nr of shoots*	*Branch age*	*Nr of trees*	*Nr of shoots*	*Branch age*
Planted pine	5	25	1-5	3	6	1, 4	3	15	1 , 3, 4
Planted spruce	5	25	1-5	3	6	1, 4	3	15	1 , 3, 4
Under-storey spruce	5	25	1-5	2	2	3	-	-	-

Table 3. Parameters of the scaling equations. The equations are of the form $Y = aX^b$. Separate values for pine and spruce are presented when they are statisitically different ($p < 0.05$).

Equation:	**Units Y**	**Units X**	**b**		**a**		**R^2**	
			Pine	**Spruce**	**Pine**	**Spruce**	**Pine**	**Spruce**
$D(L) = a_D L^u$	mm	mm	1		0.0160	0.0122	0.94	0.88
$D(\xi) \propto \xi^v$	-	-	0.237		-		0.93	
$A_L = a_N L^\gamma$	cm^2	mm	1.188	0.9645	0.760	0.437	0.92	0.63
$A_S = a_S D^{2-s}$	mm^2	mm	2-0.01	2-0.21	0.599	0.468	0.99	0.98
$d_H = a_H D^z$	µm	mm	0.307		11.152		0.90	
$K_S = a_{KH} {d_H}^w$	m Pa^{-1} s^{-1}	µm	2.432		4.716×10^{-12}		0.96	
$K_S = a_K D^{wz}$	m Pa^{-1} s^{-1}	mm	0.745		1.665×10^{-9}		0.86	

Figure captions

Figure 1. Different shoot shapes for two shoots of lengths 20 cm and 30 cm generated using Eqn (6). The exponent v determines the shape of the shoot, while u determines the between-shoot scaling of diameter *vs*. length. Cylindrical shoots ($v = 0$) and close-to-cylindrical shoots ($v = 0.3$) are assumed to follow the quarter-power scaling between shoot length and basal diameter ($u = 3/2$). If $u = v$, shoots of different length are identical along the length of the shorter shoot, while the longer one is an extension of the shorter shoot. Assuming quarter-power scaling with $u = v = 3/2$ leads to shoot diameter increasing exponentially from the apex to the base. Assuming $v = 0.5$ gives rise to paraboloid shoots, i.e., the diameter-length relationship is a parabola.

Figure 2. Sample photographs taken with an Olympus ALTRA 20 colour camera attached to an Olympus CX 31 microscope (Olympus Optical Co., Tokyo, Japan) with x400 magnification. a) pine, b) spruce in light, c) spruce in shade.

Figure 3. Scaling relationships found in the data set. See Table 3 for parameter values and goodness of fit. a) Scaling of shoot basal diameter with shoot length in the entire data set. b) Scaling of needle area with shoot length in the entire data set. c) Conduit hydraulic diameter as a function of distance from the apex. d) Conduit hydraulic diameter as a function of shoot diameter. e) Hydraulic conductivity as a function of conduit hydraulic diameter. f) Shoot conducting area as a function of shoot diameter.

Figure 4. Needle weight distribution in current shoots of pine and spruce. The shoots were divided into five segments of equal length from apex (1) to base (5). The values are means of 15 shoots.

Figure 5. Calculated (Eqn 13a) water potential in pine shoots of length 100 mm with different shapes. a) Cylindrical and paraboloid shoots. CSD = cylindrical shoot with the same diameter as the paraboloid shoots, CSV = cylindrical shoots with the same woody volume as the paraboloid shoots, PS = paraboloid shoots. Solid

lines are shoots with foliage attached at the apex, dashed lines are shoots with foliage evenly distributed along the shoot. All shoots have the same total foliage area and total transpiration rate as measured shoots of the same length. They have the same conduit diameter at shoot base as measured shoots of the same basal diameter, but no conduit widening. Note that PS with even foliage distribution overlaps with CSD with foliage at apex. b) Shoots with measured properties. Solid lines: foliage is attached to the apex, dashed lines: foliage is evenly distributed.

Figure 6. Effect of shoot length on calculated water potential loss (Eqn 13). a) Water potential at shoot apex as a function of shoot length in pine and spruce, assuming that water potential at shoot base is the same in all shoots. b) The calculated foliage-specific transpiration rate that yields the same water potential loss in shoots of all sizes.

Figure 7. Simulated effect of uneven distribution of transpiration on shoot water potential in pine. Solid line: even foliage distribution; dashed line: measured foliage distribution (Figure 4); dotted line: transpiration declines linearly from maximum at base to zero at apex with the same total transpiration as in the two previous cases; double-dashed line: transpiration declines linearly from maximum at base to zero at apex with half the total transpiration of the other cases.

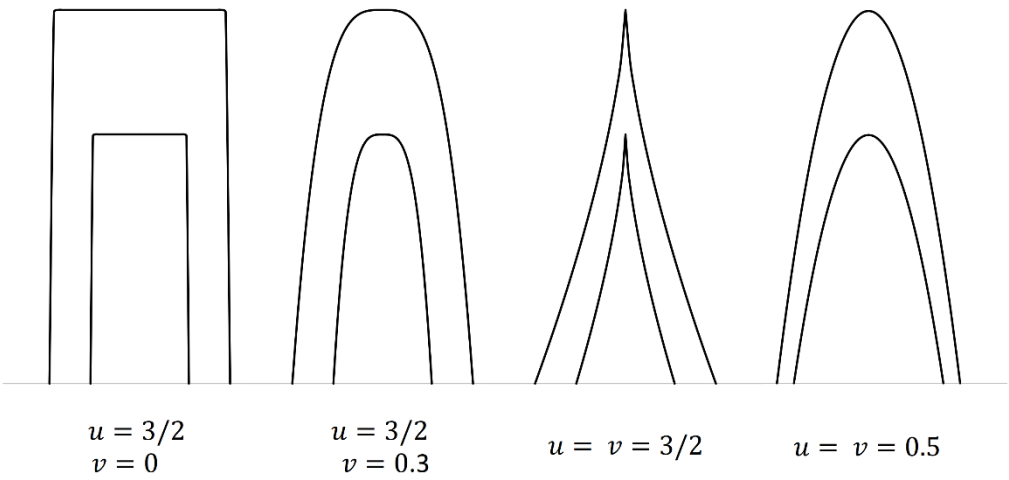

Figure 1

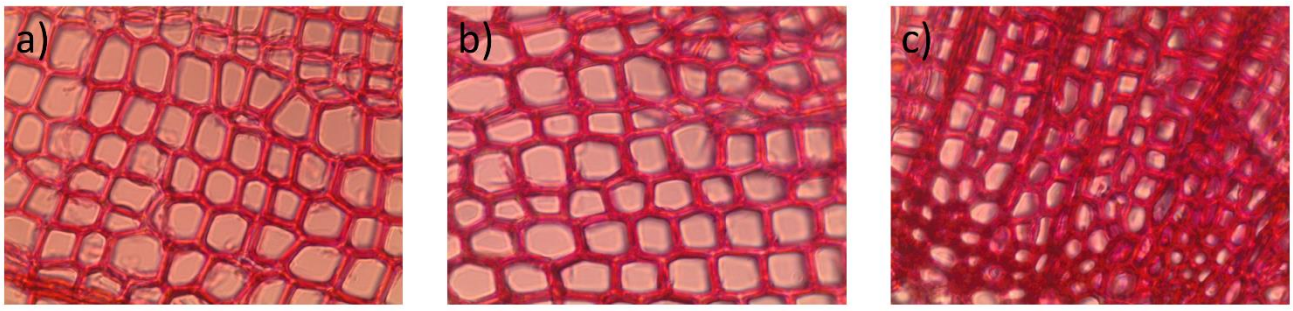

Figure 2

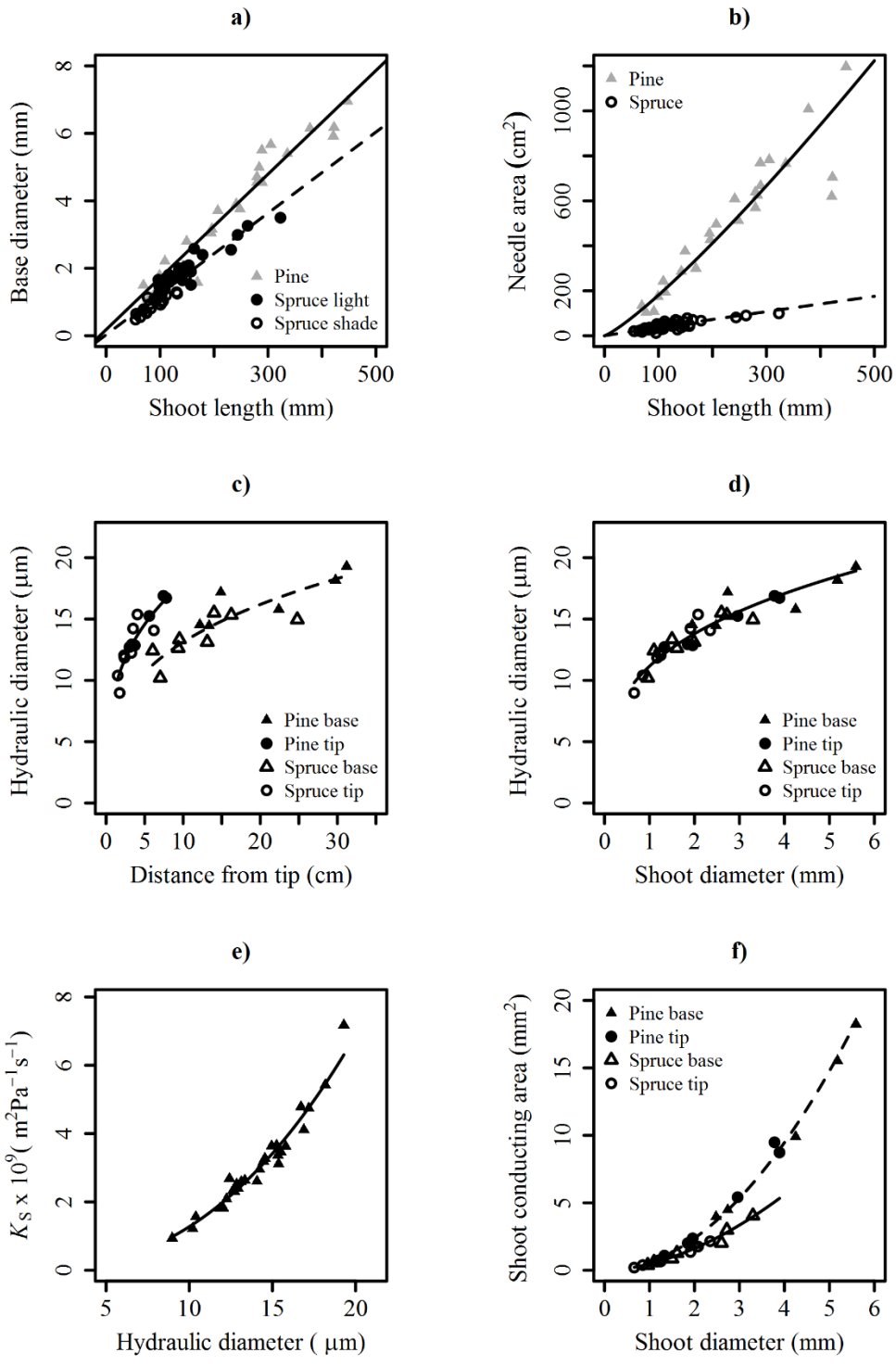
a)
Base diameter (mm)
Shoot length (mm)
Pine
Spruce light
Spruce shade
b)
Needle area (cm^2)
Shoot length (mm)
Pine
Spruce
c)
Hydraulic diameter (µm)
Distance from tip (cm)
Pine base
Pine tip
Spruce base
Spruce tip
d)
Hydraulic diameter (µm)
Shoot diameter (mm)
Pine base
Pine tip
Spruce base
Spruce tip
e)
K_S x 10^9(m^{2}Pa^{-1}s^{-1})
Hydraulic diameter (µm)
f)
Shoot conducting area (mm^2)
Shoot diameter (mm)
Pine base
Pine tip
Spruce base
Spruce tip

Figure 3

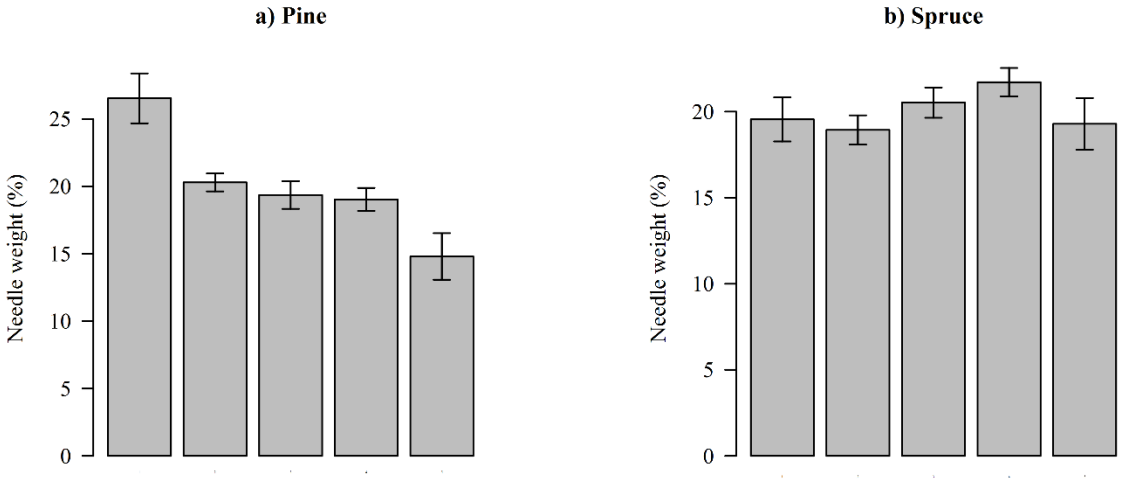

Figure 4

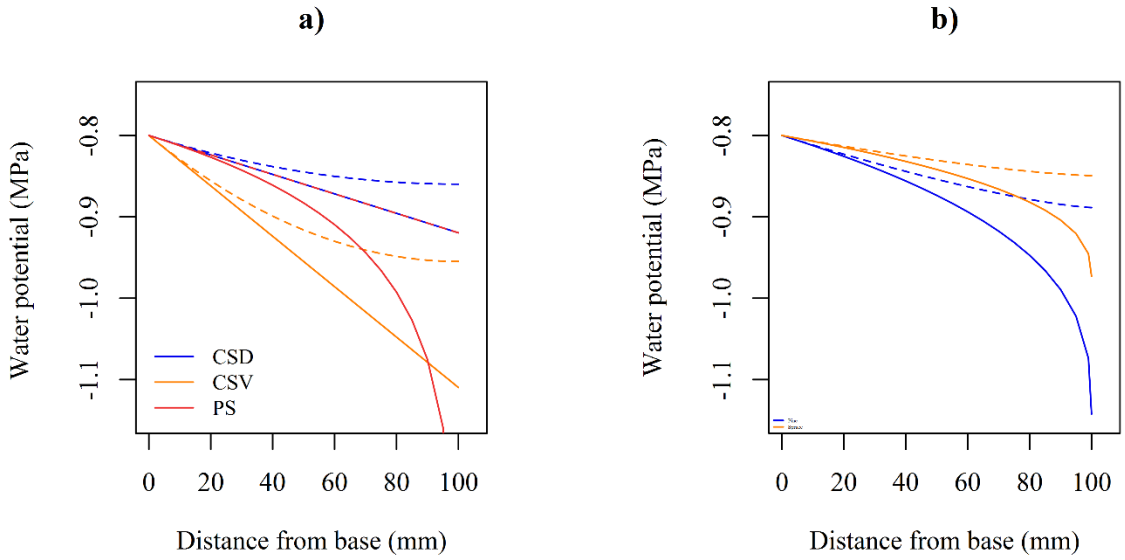

Figure 5

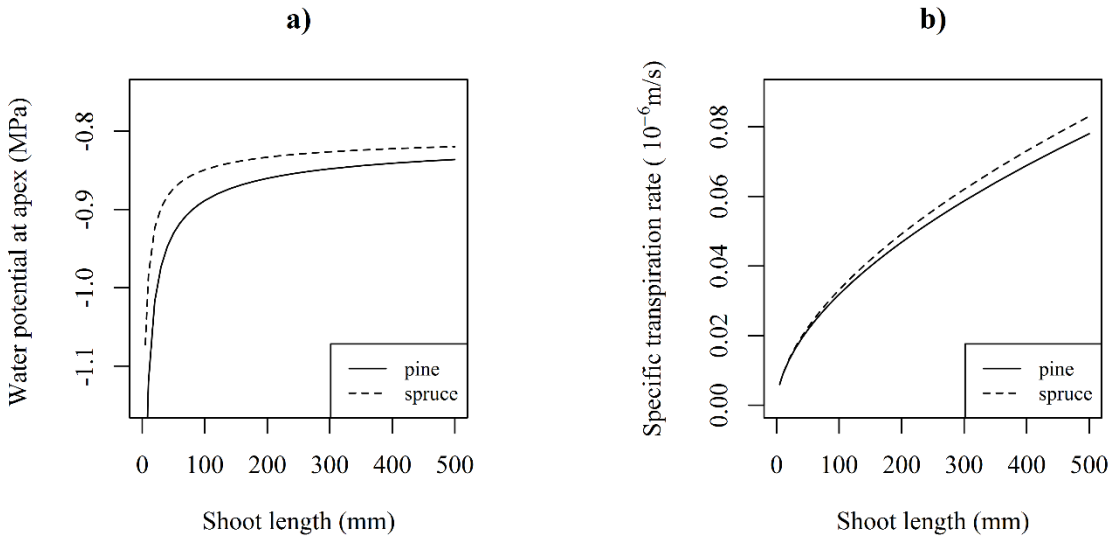

Figure 6

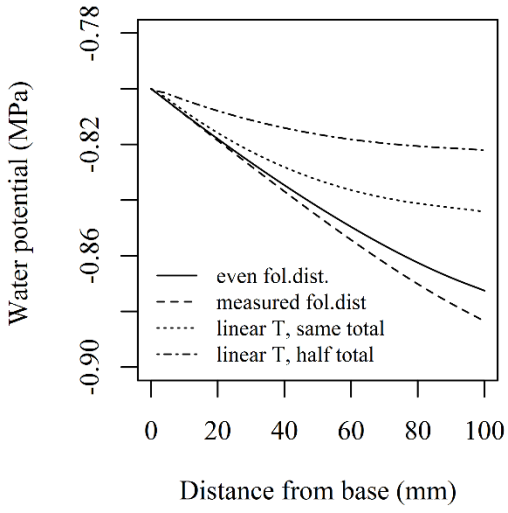

Figure 7

Supplementary material

Current-year shoot hydraulic structure in two boreal conifers – implications of growth habit on shoot water potential

Annikki Mäkelä[*)], Leila Grönlund, Pauliina Schiestl-Aalto, Tuomo Kalliokoski, Teemu Hölttä

Faculty of Agriculture and Forestry / Institute of atmospheric research and earth system science; P.O.Box 27 (Latokartanonkaari 7); 00014 University of Helsinki

[*)] corresponding author, tel: +358 41 5106515, email: annikki.makela@helsinki.fi

Supplementary material S1: Integration of shoot water potential in closed form

To integrate Eqn (4) in the text, we first convert the integration from absolute length units x to relative units ξ:

$$\frac{d\Psi}{dx} = \frac{J(x)}{A_S(x)K_S(x)} = \frac{J(L\xi)}{A_S(L\xi)K_S(L\xi)} \quad \text{(S2.1)}$$

$$\frac{d\Psi}{d\xi} = \frac{d\Psi}{dx}\frac{dx}{d\xi} = L \times \frac{J(L\xi)}{A_S(L\xi)K_S(L\xi)} \quad \text{(S3.2)}$$

The water flux inside the shoot is obtained by integration of Eqn (1) in the text:

$$\int_{J(L)}^{J(x)} dJ = \int_{L}^{x} T(x)dx = \int_{L}^{x} A_L(x)\, E dx \quad \text{(S4.3)}$$

We will solve the equation for cases where the foliage distribution is even, i.e., $A_L(x) = A_L/L$, and for cases where all the foliage is attached to the apex, i.e., $A_L(x) = 0$. In the former case we have

$$J(x) = J(L) + \frac{A_L E x}{L} - A_L E \quad \text{(S5.4)}$$

Because total transpiration is $A_L E$, this has to equal $J(L)$, i.e., the flux entering the shoot at base. Thus

$$J(x) = \frac{A_L E x}{L} = A_L E \xi \quad \text{(S6.5)}$$

For the case when the foliage is attached to the apex there is no transpiration until the apex, such that the flux remains the same as at the base, $J(x) = A_L E$. To describe bothe cases in one general form we introduce an exponent, b, that can take two values, 0 or 1, and define the flux as

$$J(x) = A_L E \xi^b \quad \text{(S7.6)}$$

Now inserting the functions in their general form into (S1.2) and accounting for all units as they occur in the regression equations we have (see Table 1):

$$\frac{d\Psi}{d\xi} = L \times 10^{-3} \times \frac{E A_L \xi^b \times 10^{-4}}{a_S[a_D L^u(\xi)^v]^{2-s} \times 10^{-6} \times a_K[a_D L^u(\xi)^v]^{wz}} \quad \text{(S8.7a)}$$

$$= L \times \frac{E a_N L^\gamma \xi^b}{a_S[a_D L^u(\xi)^v]^{2-s} \times a_K[a_D L^u(\xi)^v]^{wz}} \times 10^{-1} \quad \text{(S9.7b)}$$

$$= \frac{E a_L L^{\gamma+1} \xi^b \xi}{a_S {a_D}^{2-s} L^{u(2-s)} \xi^{v(2-s)} \times a_K {a_D}^{wz} L^{uwz} \xi^{vwz}} \times 10^{-1} \quad \text{(S10.7c)}$$

$$= \frac{E a_L L^{\gamma+1} \times 10^{-1}}{a_S {a_D}^{2-s} L^{u(2-s)} \times a_K {a_D}^{wz} L^{uwz}} \times \frac{\xi^b}{\xi^{v(2-s)} \times \xi^{vwz}} \quad \text{(S11.7d)}$$

$$= \frac{E a_L \times 10^{-1}}{a_S a_K {a_D}^{wz+2-s}} L^{\gamma+1-u(wz+2-s)} \times \xi^{b-v(wz+2-s)} \quad \text{(S12.7e)}$$

$$= \frac{E a_L \times 10^{-1}}{a_S a_K {a_D}^{wz+2-s}} L^{\gamma+1-u(wz+2-s)} \times \xi^{b-v(wz+2-s)} \quad \text{(S13.7f)}$$

$$\triangleq K(L) \times \xi^{b-v(wz+2-s)} \quad \text{(S14.7g)}$$

where we have defined $K(L)$ as the function containing the parameters and the scaling with shoot length L. This allows us to integrate the water potential gradient over the shoot:

$$\int_{\Psi(\xi)}^{\Psi(1)} d\Psi = K(L) \times \int_{\xi}^{1} \xi^{b-v(wz+2-s)} d\xi \quad \text{(S15.8a)}$$

$$= K(L) \times \frac{1}{1+b-v(wz+2-s)} \left(1 - \xi^{1+b-v(wz+2-s)}\right) \quad \text{(S16.8b)}$$

$$b - v(wz+2-s) \neq -1$$

Therefore

$$\Psi(\xi) = \Psi(1) - \frac{K(L)}{q}(1 - \xi^q) \quad \text{(S17.9)}$$

where we have denoted the exponent depending on within-shoot scaling by q:

$$q = 1 + b - v(wz + 2 - s) \quad \text{(S18.10)}$$

Particularly, we may evaluate the total water potential loss over the shoot as $\frac{K(L)}{q}$.

The case when $b - v(wz + 2 - s) = -1$ has to considered separately. In that case we have from (S1.8a):

(S19.11)

$$\int_{\Psi(\xi)}^{\Psi(1)} d\Psi = K(L) \times \int_{\xi}^{1} \frac{1}{\xi} d\xi = K(L) \times (-ln(\xi))$$

and hence

$$\Psi(\xi) = \Psi(1) + K(L)\, ln(\xi) \qquad \text{(S20.12)}$$

In this case, the total water potential loss would be infinite because $\lim_{\xi \to \infty} ln(\xi) = -\infty$ so this solution is not physically possible. However, it is the solution obtained if we assume a paraboloid shoot with foliage atteched to the apex and with no conduit tapering, i.e. $b = 0, v = 0.5, wz = s = 0$, such that

$$\xi^{b-v(wz+2-s)} = \xi^{0-0.5(0+2-0)} = \frac{1}{\xi} \qquad \text{(S21.13)}$$

Note that with conduit taper in this case, i.e., if $wz > 0$, the water potential would increase from base to apex. In order to retain a water potential gradient that would promote the flow of water towards the apex the conduits would have to widen from base to apex.

Table S1.1 summarises the scaling and size for cylindrical, paraboloid and measured shapes used in the analysis.

Table S1.1. Scaling parameters in hypothetically shaped and measured shoots. All shoots are assumed to have a constant hydraulic diameter throughout the shoot, and all have the same foliage mass and same total transpiration rate. No conduit tapering is assumed. CSED = cylindrical shoot with foliage at end, with the same basal diameter as the paraboloid shoots; CSAD = cylindrical shoot with foliage along, with the same basal diameter as the paraboloid shoots; CSEV = cylindrical shoot with foliage at end, with the same shoot volume as the paraboloid shoots; CSAV = cylindrical shoot with foliage along, with the same shoot volume as the paraboloid shoots; PSE = paraboloid shoot with foliage at end; PSA = paraboloid shoot with foliage along. MSE = measured pine shoot with foliage at end, MSA = measured pine shoot with foliage along.

Shape	b	u	v	z	w	s	γ	q	p	$D(L)$
CSED	0	1	0	0	-	0	1.188	1	0.188	$a_D L^u$
CSAD	1	1	0	0	-	0	1.188	2	0.188	$a_D L^u$
CSEV	0	1	0	0	-	0	1.188	1	0.188	$\sqrt{0.5}\, a_D L^u$
CSAV	1	1	0	0	-	0	1.188	2	0.188	$\sqrt{0.5}\, a_D L^u$
PSE	0	1	0.5	0	-	0	1.188	0	0.188	$a_D L^u$
PSA	1	1	0.5	0	-	0	1.188	1	0.188	$a_D L^u$
MSE	0	1	0.237	0.307	2.432	0	1.188	0.35	-0.57	$a_D L^u$
MSA	1	1	0.237	0.307	2.432	0	1.188	1.35	-0.57	$a_D L^u$

The size-dependence of the water potential loss can be seen from the dependence of $K(L)$ on L:

$$L^{\gamma+1-u(wz+2-s)}$$

If the exponent is positive, the water potential loss increases with size, and if it is negative, it decreases with size, so we need to study whether

$$p = \gamma + 1 - u(wz + 2 - s) < 0$$

For the measured shoots $p < 0$ for both spruce and pine (Table S1.1), whereas for the hypothetical shoots with pine parameters $p > 0$ (Table S1.1), and for spruce $p \approx 0$ because $\gamma \approx 1$ for spruce (Table 3). The difference in this case is mainly due to the fact that there is no conduit tapering in the hypothetical shoots.

For comparison, we calculate p for the WBE model (West et al. 1999) and for the Savage et al. (2010) modification (see Table 4 in text). For both of these models $u = 3/2$, $\gamma = 3$, and $z = s = 0$, so

$$p = 3 + 1 - \frac{3 \times 2}{2} = 1 > 0$$

implying that the water potential loss increases when shoot size increases. This would mean that bigger shoots would have higher hydraulic resistance than smaller shoots.

Supplementary material S2: Numerical simulation of shoot water potential

For numerical integration we used a finite element method where the shoots were divided in N numerical elements ($N = 50$) of equal length (Figure S2.1). Each numerical element was assigned a value of hydraulic conductivity and needle area according to the scaling parameters obtained in the results. The water potential loss between consecutive numerical elements was calculated as follows:

$$\Psi_i = \Psi_{i-1} - \frac{J_i l}{k_i A_i} \quad \text{when } i > 1 \qquad \text{(S2-1a)}$$

$$\Psi_1 = \Psi_{soil} - \frac{J_1}{K_{tot}} \quad \text{when } i = 1 \qquad \text{(S2-1b)}$$

where Ψ_i is water potential in element i, J_i is flow rate to element i, l is element length, k_i is conductance of element i, A_i is cross-sectional area of element *i*, K_{tot} is the leaf area specific hydraulic conductance from soil to the base of the current year shoot. The water balance for each element was solved so that

$$J_i = J_{i-1} - T_i \qquad \text{(S2-2)}$$

where T_i is the transpiration rate from element *i*. Transpirational water loss from each element was made to be proportional to needle area so that

$$T_i = A_{Li} E_i \qquad \text{(S2-3)}$$

where A_{Li} is needle area in element i and E_i is the foliage-specific transpiration rate from needle element i.

In the simulations we studied how the uneven distribution of T_i over shoot length affect the water potential values in the shoot. For this either A_{Li} or E_i were made linear functions of distance from apex.

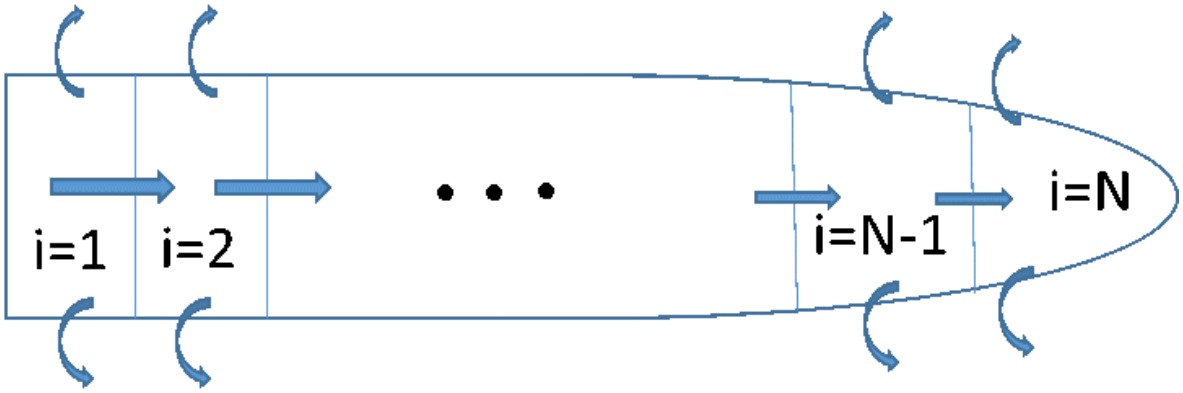

Figure S2.1. Set-up for the numerical simulation of the water flux through the shoot.

Supplementary material S3: Additional information on data.

Table S3.1. Means and standard deviations (in parentheses) of tree and shoot sizes in the data sets used. D = diameter under bark at shoot base. NA = data not available.

	Whole-shoot allometry (2014 whole set)			**Within-shoot properties** (2014 subset)			**Foliage distribution** (2017 added data)		
Species group	*Tree height (m)*	*Shoot length (mm)*	*Shoot D (mm)*	*Tree height (m)*	*Shoot length (mm)*	*Shoot D (mm)*	*Tree height (m)*	*Shoot length (mm)*	*Shoot D (mm)*
Planted pine	2.9 (0.158)	233 (46.0)	3.76 (0.635)	2.9 (0.20)	258 (139.8)	3.8 (2.096)	NA	175 (82.7)	NA
Planted spruce	3.3 (0.273)	148 (43.8)	1.93 (0.567)	3.4 (0.305)	181 (85.9)	2.21 (0.854)	NA	192 (111.2)	NA
Under-storey spruce	1.4 (0.179)	94 (44.7)	1.04 (0.599)	1.5 (0.353)	95 (8.04)	1.01 (0.127)	NA	NA	NA

Supplementary material S4: Additional scaling results.

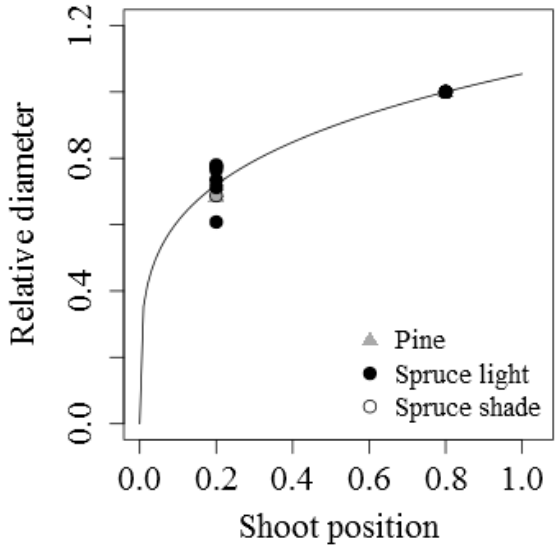

Figure S4.1 Relative shoot diameter as a function of relative distance from tip. In the data set individual shoot exponent v (Eqn 6) varies between 0.183 and 0.359, the mean being 0.237. There is no difference between spruce and pine, nor between shoots from different locations.

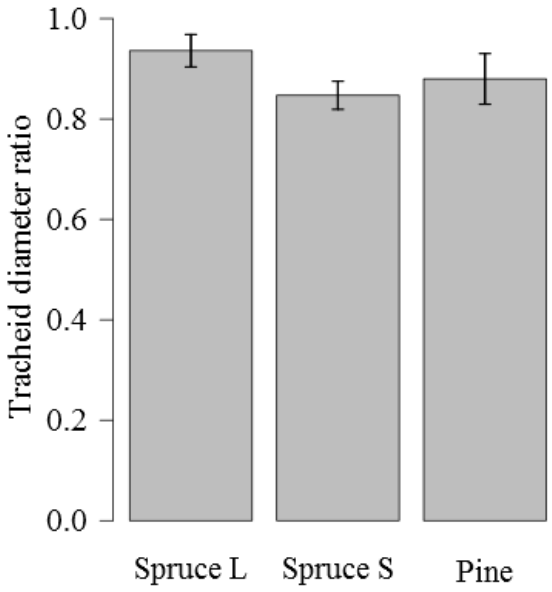

Figure S4.2. Tapering of tracheid diameter from 20% to 80% distance from base. Spruce L = spruce saplings not shaded by taller trees, Spruce S = spruce saplings as advance growth under taller canopy

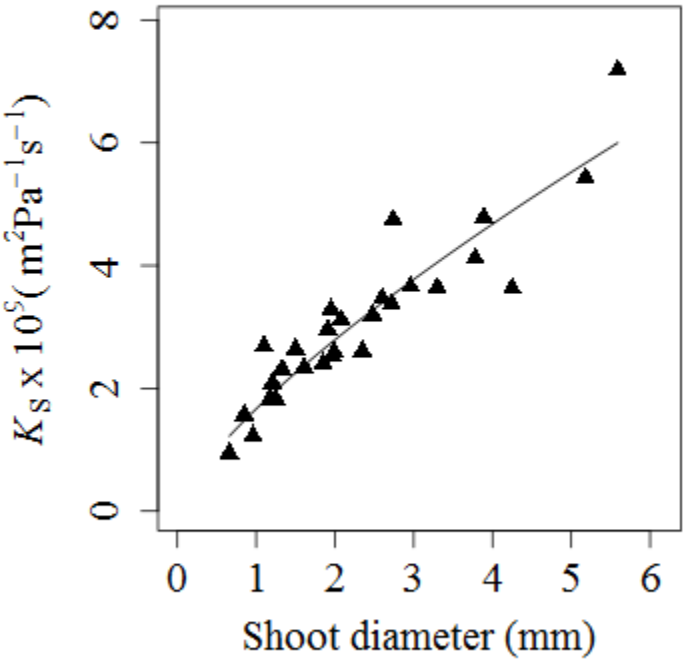

Figure S4.4. Hydraulic conductivity as a function of shoot diameter. The regression line is $K_S = 1.665 \times 10^{-9}\, D^{0.745}$, $R^2 = 0.86$.

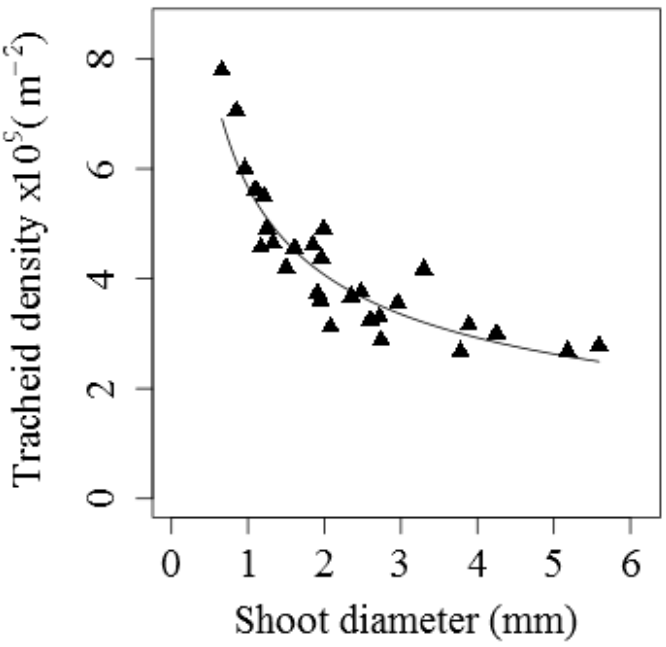

Figure S4.5. Density of conduits as a function of shoot diameter. The regression line is $y = 5.665D^{-0.477}$ ($R^2 = 0.83$).

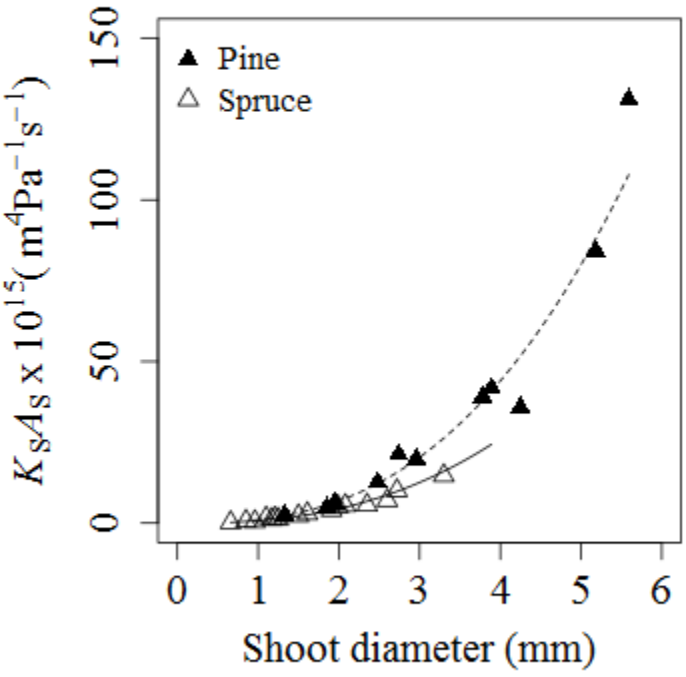

Figure S4.6. The product of conducting area and conductivity, $K_S A_S$, as a function of shoot diameter, D. The regression lines shown are those for pine ($K_S A_S = 1.076 \times (10^{-15} D^{2.677}, R^2 = 0.98$; dashed line) and spruce $K_S A_S = 0.769 \times 10^{-15} D^{2.544}, R^2 = 0.96$; solid line).

Table S4.1. Scaling exponents for current-year shoots compared with general segment scaling in some previous empricical studies and scaling theories. WBE = West et al. (1999), S = Savage et al. (2010)

Ex-ponent	Meaning	This study	Whole tree / branch measurements	Whole tree theory (WBE, S)
u	Segment ext diameter vs segment length	1	0.97 (branches; Hölttä et al. 2013)	1.5
v	External diameter vs. relative distance from apex	0.237	0.5 paraboloid 0 cylinder	0
γ	Foliage area vs segment length	1.188 (pine) 0.9645 (spruce)	2.64 (mean of conifer crowns; Duursma et al. 2010)	3
z	Conduit diameter vs ext. diameter	0.307	0.29 (0.08, 0.50) (axial and radial cross-species data; Savage et al. 2010) 0.34 (0.04, 0.64) (axial cross-species data; Savage et al. 2010) 0.236-0.292 (stem juvenile tissue, Jyske and Hölttä 2014) 0.133-0.253 (mature, Jyske and Hölttä 2014) 0.20 (0.17, 0.22; r2 = 0.55) 0.36 (Olson and Rosell 2013: self-supporting angiosperm woody species)	0.17 (WBE) 0.33 (S)
w	Sapwood-specific hydraulic conductivity vs conduit diameter	2.432	2.41 *P. sylvestris* 2.44 *P. abies* (Cochard 1992)	4 (WBE) 2 (S)
s	Ratio of conducting to non-conduction area vs ext diameter	0 (pine) -0.21 (spruce)	0.13 (-0.66, 0.92) Savage et al. 2010	0 (S) 0.33 (WBE)
wz	Area-specific segment conductivity vs ext diameter	0.746	0.55 (Scots pine stem segments; Mencuccini 2002)	0.67
	Conduit diameter vs distance from apex	0.320 (apex) 0.285 (base)	0.081 – 0.236 (Petit et al. 2008) 0.111-0.205 (juvenile, Jyske and Hölttä 2014) 0.083-0.131 (mature, Jyske and Hölttä 2014)	0.25 (WBE) 0.5 (S)
	Conduit density vs ext diameter	-0.477	-0.34 to -0.8 (conifers, Sperry et al. 2012)	-0.67 (S) 0 (WBE)
	Nr of conduits per segment vs ext diameter	1.52	1.45 (1.40, 1.49; r2 = 0.95)	1.33 (S) 2 (WBE)
	Conduit frequency vs conduit diameter	-1.55	-1.86 (-2.91, -0.81) (Savage et al. 2010)	-2 (S) 0 (WBE)